HHS Public Access

Author manuscript

Cortex. Author manuscript; available in PMC 2019 November 01.

Published in final edited form as:

Cortex. 2018 November ; 108: 222–233. doi:10.1016/j.cortex.2018.08.012.

Polarity-Dependent Modulation of Multi-Spectral Neuronal Activity by Transcranial Direct Current Stimulation

Alex I. Wiesman[1,2], **Mackenzie S. Mills**[2], **Timothy J. McDermott**[2], **Rachel K. Spooner**[1,2], **Nathan M. Coolidge**[2], and **Tony W. Wilson**[1,2]

[1]Department of Neurological Sciences, University of Nebraska Medical Center, Omaha, NE

[2]Center for Magnetoencephalography, University of Nebraska Medical Center, Omaha, NE

Abstract

The ability to preferentially deploy neural resources to the visual space is an important component of normative cognitive function, however, the population-level cortical dynamics that sub-serve this ability are not fully understood. Specifically, rhythmic activity in the occipital cortices (e.g., theta, alpha, and gamma oscillations) has been strongly implicated in this cognitive process, but these neural responses are difficult to non-invasively manipulate in a systematic manner. In this study, transcranial direct-current stimulation (tDCS) was used to modulate brain activity, while high-density magnetoencephalography (MEG) was employed to quantify changes in rhythm-specific neural activity in the occipital cortices of 57 adults performing a visuospatial processing paradigm. All MEG data was analyzed using advanced source reconstruction and oscillatory analysis methods. Our results indicated that basal levels of occipital alpha activity were increased by an occipital-anodal/supraorbital-cathodal tDCS montage, while basal gamma levels in the same cortices were decreased by tDCS using the same montage with its polarity reversed (occipital-cathodal/supraorbital-anodal). In other words, stimulation with the occipital-anodal montage increased local spontaneous alpha (10–16 Hz) activity, while stimulation with the occipital-cathodal montage selectively decreased local gamma (64–90 Hz) activity. Neither polarity affected stimulus-induced oscillations in the alpha or gamma range. Additionally, these modulations strongly predicted the subsequent formation of fronto-visual functional connectivity within distinct oscillatory rhythms, as well as behavior on the visuospatial discrimination task. These findings provide insight into the multifaceted effects of tDCS on cortical activity, as well as the dynamic oscillatory coding of salient information in the human brain.

Keywords

visual perception; oscillations; magnetoencephalography; transcranial direct current stimulation

Correspondence to: Tony W. Wilson, Center for Magnetoencephalography, 988422 Nebraska Medical Center, Omaha, Nebraska 68198-8422, twwilson@unmc.edu, Phone: (402)552-6431.

6. Declaration/Conflict of Interest:

The authors of this manuscript acknowledge no conflicts of interest, financial or otherwise.

1. Introduction

Multiple neuronal populations within the occipital cortices are known to serve visuospatial processing, and frequency-specific oscillatory neural responses among these populations have been directly linked to differing aspects of visual perception in the human brain. For example, theta (4–7 Hz) frequency oscillations have been implicated as a vital coding scheme for the temporal organization and transmission of visual stimulus sampling (Busch, Dubois, & VanRullen, 2009; Jensen & Tesche, 2002; Landau & Fries, 2012; Landau, Schreyer, van Pelt, & Fries, 2015; Verbruggen, Aron, Stevens, & Chambers, 2010), synchronization in the alpha band has been found to index the inhibition of incoming visual information in occipital regions (Handel, Haarmeier, & Jensen, 2011; Spaak, de Lange, & Jensen, 2014), and gamma (30 Hz+) activity in visual cortices is increased during visual attention (Doesburg, Roggeveen, Kitajo, & Ward, 2008; Edden, Muthukumaraswamy, Freeman, & Singh, 2009; Tallon-Baudry, Bertrand, Henaff, Isnard, & Fischer, 2005; Vidal, Chaumon, O'Regan, & Tallon-Baudry, 2006) and modulated by top-down signals from attention-related frontal areas (Baldauf & Desimone, 2014; Doesburg et al., 2008; T. R. Marshall, O'Shea, Jensen, & Bergmann, 2015). Recent work utilizing the high temporal precision of magnetoencephalography (MEG) has also found that functional connectivity between these spectrally-specific responses in occipital areas and specific prefrontal regions is important to attention function (Baldauf & Desimone, 2014; Doesburg et al., 2008; Szczepanski et al., 2014) and highly dynamic (Wiesman, Heinrichs-Graham, Proskovec, McDermott, & Wilson, 2017), although functionally dissociating these networks has proved challenging.

One potential solution to this challenge is to use neuromodulatory methods, such as transcranial direct-current stimulation (tDCS), to alter neural activity in specific brain regions. Generally speaking, tDCS creates a semi current-loop running from the anode, through the intermediate brain tissues, to the cathode following a path strongly modulated by electrical resistance. Relatively little is known regarding the effects of tDCS on neurophysiology, but early models suggest that anodal stimulation functions to decrease local GABAergic activity, thereby increasing regional neuronal excitability, while cathodal stimulation decreases local excitability through a decrease in local glutamate (Coffman, Clark, & Parasuraman, 2014; Fertonani & Miniussi, 2016; Filmer, Dux, & Mattingley, 2014; Nitsche et al., 2003; Nitsche & Paulus, 2000, 2001). However, there are other views on the source of tDCS-induced excitability changes (Jackson et al., 2016; Lafon, Rahman, Bikson, & Parra, 2017) and knowledge of the cellular and molecular neurobiology of tDCS continues to evolve. Previous systems-level studies have shown that tDCS can also modulate the neuronal and behavioral correlates of multiple cognitive domains, perhaps most prominently attention and memory (Coffman et al., 2014). Importantly, tDCS has also been found to differentially affect specific rhythms in local neuronal populations simultaneously (e.g., increase alpha and decrease gamma; Heinrichs-Graham, McDermott, Mills, Coolidge, & Wilson, 2017; T. R. Marshall, Esterer, Herring, Bergmann, & Jensen, 2016; Wilson, McDermott, Mills, Coolidge, & Heinrichs-Graham, 2018). While this capacity is potentially powerful for examining basic circuit function, little is known about how this frequency-modulation might affect visuospatial perception and related behavioral abilities. Further,

although promising, tDCS has also been found to produce extremely variable effects on cognitive performance (Hill, Fitzgerald, & Hoy, 2016; Horvath, Forte, & Carter, 2015a, 2015b; Mancuso, Ilieva, Hamilton, & Farah, 2016), and thus studies examining the spectral, temporal, and spatial alterations following stimulation are desperately needed to delineate the nature of these neural effects.

Herein, we combine tDCS and MEG to modulate and image frequency-specific population-level neuronal activity in the human brain during a visuospatial discrimination task, which has previously been shown to reliably elicit strong occipital oscillations in the theta, alpha, and gamma bands (Wiesman et al., 2017; Wiesman et al., 2018). Essentially, after stimulating the visual cortex in one of three distinct electrode configurations (i.e., occipital-anodal/supraorbital-cathodal, occipital-cathodal/supraorbital-anodal, and sham), we recorded neural activity using MEG during performance of the visuospatial task, and examined the frequency-specific modulation of visual cortical neurons by tDCS, as well as behavioral indices. Consistent with previous findings, we hypothesized that basal levels of occipital alpha activity (i.e., spontaneous alpha) would be increased by stimulation with the occipital-anodal montage (Heinrichs-Graham et al., 2017; Wilson et al., 2018), and that basal gamma levels in the same cortices would be decreased by stimulation with the occipital-cathodal montage (T. R. Marshall et al., 2016). Further, we hypothesized that functional connectivity between prefrontal and visual cortices in the theta range, found previously to sub-serve performance of this task (Wiesman et al., 2017), would be significantly modulated by tDCS, and that this modulation would impact performance and be strongly affected by the polarity of stimulation.

2. Methods:

2.1 Participants

We enrolled 57 healthy adults (54 right-handed; 33 males) for this study. All participants were between the ages of 20 and 32 years (Mean = 24.04; SD = 2.78). Exclusionary criteria included any medical illness affecting CNS function (e.g., HIV/AIDS), any neurological disorder, history of head trauma, and current substance abuse. The Institutional Review Board of the University of Nebraska Medical Center reviewed and approved this investigation. Written informed consent was obtained from each participant following a detailed description of the study. Once participants were consented, they were randomly assigned to sham (21 participants, 8 female), occipital-anodal/supraorbital-cathodal montage (19 participants, 8 female), and occipital-cathodal/supraorbital-anodal (17 participants, 8 female) montage groups. A between-subjects design was selected for this study, to rule out any potential learning and longer-term after-effects that might be introduced by a repeated measures design. Such between-subjects experimental designs are relatively standard in major clinical trials, especially for pharmaceuticals. Participants were blinded to their group identification, as were all researchers associated with data analyses. The three groups did not statistically differ on age (sham: 23.86 years; occipital-anodal montage: 24.42 years; occipital-cathodal montage: 23.75 years), sex, handedness, ethnicity, or educational level. With the exception of stimulation condition, all participants completed the same experimental protocol. Importantly, MEG data collected during two different cognitive tasks

completed by the participants assigned to the occipital-anodal and sham montage groups has been analyzed and reported previously (Heinrichs-Graham et al., 2017; Wilson et al., 2018), although for these studies participants performed only passive viewing of stimuli. Thus, the MEG and behavioral data reported here is 100% new and not included in the previous studies.

2.2 Transcranial Direct Current Stimulation (tDCS)

Across all three groups, a 5 × 7 cm pad was positioned over midline occipital cortex near the calcarine fissure, and a second 5 × 7 cm pad was positioned over the right prefrontal cortices near the area generally referred to as supraorbital in most tDCS studies (Figure 1A). Each tDCS sponge was soaked in saline solution and positioned on the head using the International 10/20 system (Jasper, 1958), which is commonly employed in EEG, fNIRS, and tDCS studies (e.g., Wilson, Kurz, & Arpin, 2014). In our experiment, the occipital pad was positioned on the midline and centered about 12.5% above the inion, which corresponds to ~2.5% superior to Oz. The right frontal pad was centered directly lateral to Fp2 by ~7.5%, which is one of the most common areas for cathodal placement (Filmer et al., 2014). Importantly, Okamoto et al. (Okamoto et al., 2004; Okamoto & Dan, 2005) have developed a method for transforming the scalp-based International 10–20 coordinate system to Montreal Neurological Institute (MNI) based coordinates. Briefly, using data from a large sample of healthy adults, they developed a probabilistic distribution of the cortical projection points in MNI space that corresponds to input coordinates from the International 10–20 system. Based on their data, coordinates in the International 10–20 system (i.e., scalp-based) can be estimated in MNI space with an average standard deviation of 8 mm, which is negligible given the size of our tDCS sponges. Thus, we computed the coordinates of each sponge in the International 10–20 system, and then used the transformation methods provided by Okamoto et al. to obtain the MNI coordinates that corresponded to these scalp based locations. These data indicated that the occipital pad was near the calcarine fissure, while the frontal pad was over right supraorbital cortices. For the occipital-anodal montage, the midline occipital pad served as the anode and the supraorbital pad served as the cathode. For the occipital-cathodal montage, the polarity was reversed so that the midline occipital pad served as the cathode, while the anode was positioned over the right supraorbital. In the sham condition, the sponges were in the same locations but were only briefly activated (see below).

Participants in each active stimulation group (i.e., the occipital-anodal and occipital-cathodal montages) underwent 20 minutes of 2.0 mA direct-current stimulation, plus ~30 s ramp-up and ramp-down periods, while passively viewing an animated movie. Three dimensional current density modeling of this stimulation was performed using finite-element modeling (FEM) of current flow to verify that the occipital cortices were being targeted effectively (Kempe, Huang, & Parra, 2014; Ruffini, Fox, Ripolles, Miranda, & Pascual-Leone, 2014). The sham group received the same passive visual experience for 20 minutes, but no stimulation outside of the ~30 s ramp periods. A Soterix Medical (New York, New York, USA) tDCS system was used for stimulation. Following active/sham stimulation, participants were prepared for MEG recording and seated with their head positioned within the MEG helmet. The overall setup took about 45 minutes from the stop of stimulation to the

initiation of the MEG session, which was by design given the findings of Kuo et al. (Kuo et al., 2013). Briefly, this study found that the level of cortical excitability peaks about 20 minutes after the cessation of tDCS, and then slowly dissipates over the next 70 to 90 minutes. Consistent with these data, Bachtiar et al. (Bachtiar, Near, Johansen-Berg, & Stagg, 2015) reported that local GABA decreases following 20 minutes of anodal tDCS peaked about 20 minutes after stimulation, and remained decreased for an extended time period thereafter. Thus, we aligned our MEG recording session to coincide with this period of heightened neuronal excitability.

2.3 MEG Experimental Paradigm

The paradigm used was an established visuospatial discrimination task intended to tap visual perceptual processing (Figure 1C; Wiesman et al., 2017; Wiesman et al., 2018). During this task, the participants were seated and told to fixate on a crosshair presented centrally. After a variable ISI (range: 1900–2100 ms), an 8×8 grid was presented for 800 ms at one of four positions relative to the fixation: above right, below right, above left, or below and to the left (Figure 1C). The left/right orientations were defined as a lateral offset of 75% of the grid from the center of fixation. Before the task began, participants were instructed to respond via button press with their right hand whether the grid was positioned to the left (index finger) or right (middle finger) of the fixation point upon presentation of the grid. The task was designed to be easy enough for all participants to have high accuracy, while demanding enough to require sustained attention to the visual stimulus throughout the recording. Each participant performed 240 repetitions of the task concurrent with MEG recording.

2.4 MEG Data Acquisition

All recordings were conducted in a one-layer magnetically-shielded room with active shielding engaged for environmental noise compensation. With an acquisition bandwidth of 0.1– 330 Hz, neuromagnetic responses were sampled continuously at 1 kHz using an Elekta MEG system (Helsinki, Finland) with 306 sensors, including 204 planar gradiometers and 102 magnetometers.. Each MEG dataset was individually corrected for head motion and subjected to noise reduction using the signal space separation method with a temporal extension (Taulu & Simola, 2006).

2.5 MEG Coregistration with Anatomy & Data Pre-Processing

MEG data were preprocessed using an established pipeline (Heinrichs-Graham, McDermott, Mills, Coolidge, & Wilson, 2016; Kurz, Wiesman, Coolidge, & Wilson, 2017; McDermott, Wiesman, Proskovec, Heinrichs-Graham, & Wilson, 2017; Wiesman, Heinrichs-Graham, McDermott, et al., 2016; Wilson et al., 2018; Wilson et al., 2017), which included coregisteration to structural MRIs, epoching around stimulus onset (−400 to 2200 ms), rejection of artifacts, transformation into the time-frequency domain, and non-parametric permutation testing (Ernst, 2004; Maris & Oostenveld, 2007) to identify the MEG sensor-level time-frequency windows with significant changes relative to the baseline. After artifact rejection, an average of 217.11 (SD = 6.36) trials per participant were used for further analysis, and the mean number of trials per participant did not differ by group (sham: 219.43; occipital-anodal montage: 215.79; occipital-cathodal montage: 215.63; $p > 0.1$).

2.6 MEG Source Imaging and Statistics

Cortical networks were imaged through an extension of the linearly constrained minimum variance vector beamformer (Gross et al., 2001). Grand averages were then computed using the pseudo-t maps from all participants, consistent with established methodology (Cheyne, Bakhtazad, & Gaetz, 2006; Jurkiewicz, Gaetz, Bostan, & Cheyne, 2006; Kurz et al., 2017; Wiesman, Heinrichs-Graham, Coolidge, et al., 2016; Wiesman, Heinrichs-Graham, McDermott, et al., 2016). Virtual sensors (i.e., voxel time series) were then computed from the peak voxel of each cluster in the occipital cortices, which was defined as the voxel with the maximum amplitude value within each spatially defined cluster. Since theta activity in the bilateral inferior frontal cortices was previously found to be essential to performance of this task (Wiesman et al., 2017), we also computed virtual sensors for these regions, using MNI coordinates corresponding to the peak voxel from that experiment. **The same coordinates were used for all participants**.

Virtual sensors were computed by applying the sensor weighting matrix derived through the forward computation to the preprocessed signal vector, which yielded a time series for the specific coordinate in source space. Note that virtual sensor extraction was done per participant individually, once the coordinates of interest were known. To determine whether stimulation condition significantly affected basal levels of activity at each spatially- and spectrally-defined peak, values from the absolute amplitude time series from each peak were averaged across the baseline period (−400 to 0 ms). Further, to probe whether task-related responses (relative to baseline) were significantly modulated by stimulation condition, values from the relative amplitude time series from each peak were averaged across the task-active period, defined as the time window from onset of the visual stimulus to the time bin preceding the mean reaction time across all participants (0 to 500 ms). Since no effect of hemisphere was hypothesized, bilateral activity values were averaged within participants. These computed values were then compared between groups using one-way ANOVAs, with post-hoc testing using Fisher's LSD. For all statistical testing, outliers were excluded based on a fixed threshold of ± two standard deviations from the mean.

2.7 Functional Connectivity Analyses

In order to evaluate dynamic connectivity between visual perception-related neural regions, we computed phase coherence within the respective frequency bands of our statistically-defined clusters. To compute phase coherence, we extracted the phase-locking value (PLV) using the method described by Lachaux et al (Lachaux, Rodriguez, Martinerie, & Varela, 1999). The PLV reflects the inter-trial variability of the phase relationship between pairs of brain regions as a function of time. Values close to 1 indicate strong synchronicity (i.e. phase-locking) between the two brain regions within the specific time window across trials, whereas values close to 0 indicate substantial phase variation between the two signals, and thus, weak synchronicity (connectivity) between the two regions. To determine whether task-related functional connectivity differed significantly between groups, values from the extracted PLV time series per pair of peaks were averaged across the task-active period. No effect of hemisphere for visual responses was hypothesized, however extensive literature substantiates the functional laterality of the prefrontal cortices. To account for this, task-active PLV values were averaged within participants across the visual sources, but not across

the frontal sources. These values were then compared using one-way ANOVAs, with post-hoc testing using Fisher's LSD. Once again, outliers were excluded based upon a fixed threshold of ± two standard deviations from the mean.

2.8 Linear Regression Analyses

To examine the hypothesized predictive capacity of basal (baseline) neural activity on task performance, linear regression models were computed using reaction time and accuracy, respectively, on basal amplitude in the alpha and gamma frequency bands. Further, a linear regression of right inferior frontal-visual PLV on basal alpha amplitude was also computed, to determine whether modulations in alpha activity affected dynamic communication in the brain. All regression analyses were performed in SPSS (Chicago, Illinois, USA).

3. Results:

3.1 Current Modeling and Behavioral Effects

Participants were stimulated using one of three current configurations (i.e., an occipital-anodal montage, an occipital-cathodal montage, or sham; see Methods), with each having an identical spatial configuration for electrode placement (Figure 1A; see Figure S1 for experimental design). Three-dimensional current distribution modeling showed that the field intensity was strongest in occipital cortex for both occipital-anodal and occipital-cathodal configurations, particularly around the occipital poles (Figure 1B). After stimulation, participants completed a visuospatial discrimination task (Figure 1C) during MEG, which had been previously shown to elicit robust, multi-spectral activity in occipital cortices (Wiesman et al., 2017; Wiesman et al., 2018). In regard to behavioral performance, a significant effect of group was observed for task accuracy (Figure 1D; $F(2,50) = 6.20$, $p = .004$), and post-hoc analyses revealed that participants who received stimulation with the occipital-anodal montage were significantly less accurate than participants stimulated with the occipital-cathodal montage and participants in the sham group ($p < .05$). No main effect of group was found for reaction time (Figure 1D), although a strong trend was observed ($F(2,50) = 2.93$, $p = .063$), and follow-on t-tests revealed that participants stimulated with the occipital-anodal montage were significantly slower than participants who received sham tDCS ($p < .05$).

3.2 Frequency-specific Responses in Visual Processing Circuits

One participant in the occipital-cathodal montage group was excluded from all analyses due to a technical error during the MEG recording, leaving a remaining 56 participants in total (53 right-handed; 32 males). In agreement with previous studies, presentation of the visual stimulus elicited robust oscillations in the occipital cortices across three distinct rhythms (Figure 2). The specific time-frequency windows for follow-on analyses were determined using stringent statistical methods (Figure S2). Specifically, in bilateral parieto-occipital sensors, an early, transient increase in neural-ensemble activity occurred in the theta (4–8 Hz) range between 100 and 350 ms, and this was followed by a more sustained decrease in alpha power (10–16 Hz) between 150 and 750 ms (Figure 2B, lower). Concurrent with these lower frequency oscillations, power in the gamma range (64–90 Hz) increased in sensors more posterior between 100 and 600 ms (Figure 2B, upper). To clarify the potential impact

of evoked activity on the theta and alpha responses, we re-ran these analyses after removing the evoked signal and the results remained the same. The same was true for the virtual sensor analyses described below.

We next investigated the spatial origin of these sensor-level responses using a beamformer. The robust decrease in alpha power was found to have originated in bilateral parieto-occipital regions, while the theta and gamma increases were generated by more posterior-medial primary visual areas (Figure S3). Virtual sensors (i.e., voxel time series) were computed for the peak voxel in each of these bilateral regions, which subsequently allowed us to examine the evolution of these responses on a precise temporal scale. Due to the importance of theta coupling between frontal and parieto-occipital nodes during attention-demanding visual tasks, (Fellrath, Mottaz, Schnider, Guggisberg, & Ptak, 2016; Kwon, Watanabe, Fischer, & Bartels, 2017; Liebe, Hoerzer, Logothetis, & Rainer, 2012; Wiesman et al., 2017) we also computed dynamic phase coherence between inferior frontal and primary visual nodes at this bandwidth (Figure S4).

3.3 Frequency-specific tDCS Modulation of Basal Neuronal Activity

Once we had identified the brain regions and circuits involved in processing of the visuospatial stimulus, we examined the effects of tDCS on these dynamics. Importantly, we examined how the different stimulation montages (polarities) affected not only the dynamics following the onset of the stimulus, but also the spontaneous levels of neural activity in these "task-relevant" regions prior to the onset of the stimulus. This is essential, as we have shown in previous studies that changes in spontaneous activity during the baseline often affect the amplitude of neural oscillations in response to a stimulus (Heinrichs-Graham & Wilson, 2016; Wilson, Heinrichs-Graham, & Becker, 2014). Stimulation with both the occipital-anodal and occipital-cathodal montages significantly altered basal amplitude (i.e., spontaneous activity during the baseline) in occipital regions, but intriguingly they did so in opposing directions and within distinct rhythms (Figure 3, bottom). Specifically, a significant effect of group was found for basal alpha amplitude ($F(2,48) = 4.22$, $p = .021$) in lateral occipital regions, and post-hoc analyses revealed that participants stimulated with the occipital-anodal montage exhibited increased basal alpha during the baseline relative to those who received stimulation with the occipital-cathodal and sham montages ($p < .05$). A significant effect of group was also found in basal gamma levels ($F(2,50) = 11.44$, $p < .001$) within primary visual cortices, but in contrast to the alpha findings it was driven by stimulation with the occipital-cathodal montage and reflected *decreased* basal gamma during the baseline compared to stimulation with both the occipital-anodal montage and sham ($p < .05$). Importantly, these modulations were frequency-specific, as basal activity in the occipital cortices at another critical bandwidth, theta, was unaltered by either stimulation montage. Further, these modulations were specific to spontaneous or resting (i.e., basal) activity, as there was no significant effect of group on oscillatory responses following the onset of the visual stimuli in any of these frequency bands (Figure S5).

To determine whether the basal neural activity differences predicted behavioral performance on the visual processing task, we computed a linear regression of accuracy and reaction time on basal amplitude levels for all participants using the gamma, alpha, and theta data.

Spontaneous alpha amplitude significantly predicted reaction time ($F(1,46) = 10.35$, $p = .002$, $R = .43$; Figure 4A), such that as basal alpha increased, so did reaction time (i.e., more alpha was related to worse behavioral performance). Basal amplitude in the theta band also predicted reaction time ($F(1,46) = 7.90$, $p = .007$, $R = .39$; Figure 4B), such that as spontaneous theta increased, so did reaction time. In contrast, basal gamma did not significantly predict reaction time. Neither basal theta, alpha, nor gamma activity levels significantly predicted accuracy on the task.

3.4 tDCS Modulation of Dynamic Functional Connectivity

In contrast to the negative basal amplitude findings for theta, phase coherence in the theta range was significantly modulated by both stimulation conditions (Figure 5) during the visual processing period. Specifically, a significant effect of group was found in fronto-visual connectivity involving the right ($F(2,50) = 5.40$, $p = .008$), but not the left, inferior frontal cortices. Post-hoc testing revealed significantly weaker functional connectivity between the right inferior frontal cortex and the right and left visual cortices following onset of the visual stimulus in the group stimulated with the occipital-anodal montage compared to those stimulated with the occipital-cathodal montage and the sham group ($p < .05$). Bilateral functional connectivity between inferior frontal nodes was also significantly modulated by stimulation ($F(2,50) = 5.82$, $p = .005$), and post-hoc analyses revealed that the participants stimulated with the occipital- cathodal montage had increased functional connectivity during visual processing, as compared to those stimulated with the occipital-anodal montage or the sham group ($p < .05$).

Finally, since increased alpha activity is thought to act as an inhibitor of incoming visual information (Jensen & Mazaheri, 2010), it is possible that high basal alpha activity in visual cortices, prior to the onset of the visual stimulus, would impair the dynamic functional connections formed between these cortices and other regions during visual processing. To test this hypothesis, we computed linear regressions of theta functional connectivity between the right inferior frontal cortex and the bilateral primary visual cortices on alpha basal amplitude levels. As expected, basal alpha levels did significantly predict functional connectivity ($F(1,47) = 5.15$, $p = .028$, $R = -.31$; Figure 6).

4. Discussion:

By stimulating the cortex with tDCS and imaging the resulting neural modulations with MEG, we have demonstrated that frequency-specific neural activity sub-serving visuospatial processing can be differentially modulated depending on the local polarity of tDCS, and that this modulation also has rhythm-specific effects on behavior. In particular, stimulation with the occipital-anodal montage significantly increased basal alpha activity during the pre-stimulus baseline (i.e., spontaneous alpha), and the amplitude of such alpha activity strongly predicted one's ability to discriminate the position of stimuli in visual space. In contrast, basal gamma was only modulated by stimulation with the occipital-cathodal montage, and this involved a significant decrease in spontaneous gamma that was not predictive of task performance. Finally, theta activity in occipital cortices was found to be unaffected by tDCS, highlighting the spectral-specificity of these modulations. In addition, we showed that

transient functional connections in the theta band were differentially affected by the stimulation montage, and that functional connections in the theta range formed with visual cortices were impacted by basal modulations at a different frequency (alpha).

The notion that tDCS modulates distinct population-level neuronal rhythms is supported by a breadth of literature (Groppa et al., 2010; Hanley, Singh, & McGonigle, 2016; Heinrichs-Graham et al., 2016; Hsu, Tseng, Liang, Cheng, & Juan, 2014; L. Marshall, Mölle, Hallschmid, & Born, 2004; T. R. Marshall et al., 2016; Wilson et al., 2018), however few studies have demonstrated this effect dissociably within a single experiment (i.e., modulated two distinct frequencies simultaneously). Further, until now it has remained unclear how these frequency-specific effects relate to behavioral performance, or to the dynamic changes in functional connectivity that sub-serve complex cognitive processes such as visuospatial perception. Since heightened levels of alpha activity have been reliably found to represent an endogenous source of inhibition in the visual pathway (Foxe & Snyder, 2011; Handel et al., 2011; Kelly, Lalor, Reilly, & Foxe, 2006; Klimesch, 2012; Klimesch, Sauseng, & Hanslmayr, 2007; Spaak et al., 2014; van Dijk, Schoffelen, Oostenveld, & Jensen, 2008; Worden, Foxe, Wang, & Simpson, 2000), it is intuitive that the observed elevations in basal alpha levels would predict reaction time on our task, signaling heightened inhibition within the visual pathway upon presentation of task-relevant stimuli. Indeed, similar findings of impaired behavioral performance due to heightened pre-stimulus alpha activity have been reported previously (Hanslmayr et al., 2007; Romei, Brodbeck, et al., 2008; Romei, Gross, & Thut, 2010; Romei, Rihs, Brodbeck, & Thut, 2008). Interestingly, such alpha changes in our study also affected the ability of these cortices to functionally interact with higher-order frontal regions. There are at least two possible explanations for this finding: either the oscillatory dynamics of increased alpha levels act to functionally inhibit the transmission of information in a neighboring frequency band (theta; e.g., through signal leakage), or diminished stimulus representations in the visual cortices (caused by alpha inhibition) require less phase synchronization for information transfer. Further study is required to fully elucidate this process, but in either case the functional result is the same; increased spontaneous alpha activity in occipital cortices hinders the formation of functional connections with frontal regions.

The reduction we observed in basal gamma-frequency activity following stimulation with the occipital-cathodal montage is also a very pertinent finding, although this modulation had no significant relationship to behavior. This may be a result of the task design, as gamma oscillations are most commonly associated with appraisal of stimulus representations (Busch, Debener, Kranczioch, Engel, & Herrmann, 2004; Hoogenboom, Schoffelen, Oostenveld, Parkes, & Fries, 2006; Muthukumaraswamy & Singh, 2013; Siegel, Donner, Oostenveld, Fries, & Engel, 2007), and our task required only the localization of stimuli in visual space (as opposed to the appraisal of the stimuli themselves). Thus, the inhibition of these representations would not likely have affected our behavioral outcomes as robustly.

Dynamic functional connectivity between bilateral frontal and fronto-visual cortices in the theta band has been found to support the deployment of neural resources to the visual space (Wiesman et al., 2017). In this study, we found that the formation of these transient connections is modulated by transcranial stimulation, and that a likely cause of this altered

functional connectivity is elevated basal alpha activity levels in visual cortex. Since theta-frequency activity is commonly associated with the temporal organization of lower-order stimulus information, and the right inferior frontal cortex with integration of lower and higher order information processing (Fox, Corbetta, Snyder, Vincent, & Raichle, 2006; He et al., 2007; Wiesman et al., 2017), this disruption by tDCS likely signals a transient deficiency in the participants' ability to transfer salient stimulus information to higher-order regions involved in cognitive control.

Although these findings are intriguing, this research is not without limitations. For one, with a between-groups study design it is never possible to *completely* rule out the possibility of pre-existing differences between groups. This concern is at least partially mitigated by our careful counterbalancing of groups on important demographic factors such as age and education. Further, due to the position of our "reference electrode" over the supraorbital, there remains the possibility for confounding retinal stimulation effects. Although to our knowledge no long-lasting effects of retinal stimulation on visual perception have been reported, this remains a possible confound. This research also does not investigate the potential effects of tDCS on anticipatory networks, which are intimately linked with the processing of visual perception and attention. Future studies should follow this line of inquiry. Finally, although the effects reported here are intriguing, due to the relative lack of research examining the effects of tDCS on neural oscillations, they remain relatively unexplained at this time. Additional studies will be essential, not only to replicate these results, but also to investigate their underlying mechanisms at the cell-circuit and bio-molecular levels.

En masse, our findings highlight the dynamic, multi-spectral nature of visuospatial processing in the human brain, as well as the multifaceted effects of transcranial electrical stimulation on these systems. Importantly, until now, no studies have demonstrated frequency-specific, dissociable modulation of these systems using parallel experimental methods, and so the experimental procedure documented here may prove invaluable to future research focusing on multi-spectral activity in the visual cortex.

Supplementary Material

Refer to Web version on PubMed Central for supplementary material.

Acknowledgements:

This research was supported by grants R01-MH103220 (TWW), R01-MH116782 (TWW), RF1-MH117032 (TWW), and F31-AG055332 (AIW) from the National Institutes of Health, grant #1539067 from the National Science Foundation (TWW), the Shoemaker Prize from the University of Nebraska Foundation (TWW), and a grant from the Nebraska Banker's Association (TWW).

7. References:

Bachtiar V, Near J, Johansen-Berg H, & Stagg CJ (2015). Modulation of GABA and resting state functional connectivity by transcranial direct current stimulation. Elife, 4, e08789. doi:10.7554/eLife.08789 [PubMed: 26381352]

Baldauf D, & Desimone R (2014). Neural mechanisms of object-based attention. Science, 344(6182), 424–427. doi: 10.1126/science.1247003 [PubMed: 24763592]

Busch NA, Debener S, Kranczioch C, Engel AK, & Herrmann CS (2004). Size matters: effects of stimulus size, duration and eccentricity on the visual gamma-band response. Clin Neurophysiol, 115(8), 1810–1820. doi: 10.1016/j.clinph.2004.03.015 [PubMed: 15261860]

Busch NA, Dubois J, & VanRullen R (2009). The phase of ongoing EEG oscillations predicts visual perception. J Neurosci, 29(24), 7869–7876. doi: 10.1523/JNEUROSCI.0113-09.2009 [PubMed: 19535598]

Cheyne D, Bakhtazad L, & Gaetz W (2006). Spatiotemporal mapping of cortical activity accompanying voluntary movements using an event-related beamforming approach. Hum Brain Mapp, 27(3), 213–229. doi:10.1002/hbm.20178 [PubMed: 16037985]

Coffman BA, Clark VP, & Parasuraman R (2014). Battery powered thought: enhancement of attention, learning, and memory in healthy adults using transcranial direct current stimulation. Neuroimage, 85 Pt 3, 895–908. doi: 10.1016/j.neuroimage.2013.07.083 [PubMed: 23933040]

Doesburg SM, Roggeveen AB, Kitajo K, & Ward LM (2008). Large-scale gamma-band phase synchronization and selective attention. Cereb Cortex, 18(2), 386–396. doi: 10.1093/cercor/bhm073 [PubMed: 17556771]

Edden RA, Muthukumaraswamy SD, Freeman TC, & Singh KD (2009). Orientation discrimination performance is predicted by GABA concentration and gamma oscillation frequency in human primary visual cortex. J Neurosci, 29(50), 15721–15726. doi:10.1523/JNEUROSCI.4426-09.2009 [PubMed: 20016087]

Ernst MD (2004). Permutation methods: a basis for exact inference. Statistical Science, 19(4), 676–685.

Fellrath J, Mottaz A, Schnider A, Guggisberg AG, & Ptak R (2016). Theta-band functional connectivity in the dorsal fronto-parietal network predicts goal-directed attention. Neuropsychologia, 92, 20–30. doi: 10.1016/j.neuropsychologia.2016.07.012 [PubMed: 27422540]

Fertonani A, & Miniussi C (2016). Transcranial Electrical Stimulation: What We Know and Do Not Know About Mechanisms. Neuroscientist. doi: 10.1177/1073858416631966

Filmer HL, Dux PE, & Mattingley JB (2014). Applications of transcranial direct current stimulation for understanding brain function. Trends Neurosci, 37(12), 742–753. doi:10.1016/j.tins.2014.08.003 [PubMed: 25189102]

Fox MD, Corbetta M, Snyder AZ, Vincent JL, & Raichle ME (2006). Spontaneous neuronal activity distinguishes human dorsal and ventral attention systems. Proc Natl Acad Sci U S A, 103(26), 10046–10051. doi: 10.1073/pnas.0604187103 [PubMed: 16788060]

Foxe JJ, & Snyder AC (2011). The Role of Alpha-Band Brain Oscillations as a Sensory Suppression Mechanism during Selective Attention. Front Psychol, 2, 154. doi: 10.3389/fpsyg.2011.00154 [PubMed: 21779269]

Groppa S, Bergmann TO, Siems C, Mölle M, Marshall L, & Siebner HR (2010). Slow-oscillatory transcranial direct current stimulation can induce bidirectional shifts in motor cortical excitability in awake humans. Neuroscience, 166(4), 1219–1225. doi: 10.1016/j.neuroscience.2010.01.019 [PubMed: 20083166]

Gross J, Kujala J, Hamalainen M, Timmermann L, Schnitzler A, & Salmelin R (2001). Dynamic imaging of coherent sources: Studying neural interactions in the human brain. Proc Natl Acad Sci U S A, 98(2), 694–699. doi: 10.1073/pnas.98.2.694 [PubMed: 11209067]

Handel BF, Haarmeier T, & Jensen O (2011). Alpha oscillations correlate with the successful inhibition of unattended stimuli. J Cogn Neurosci, 23(9), 2494–2502. doi: 10.1162/jocn.2010.21557 [PubMed: 20681750]

Hanley CJ, Singh KD, & McGonigle DJ (2016). Transcranial modulation of brain oscillatory responses: A concurrent tDCS-MEG investigation. Neuroimage, 140, 20–32. doi:10.1016/j.neuroimage.2015.12.021 [PubMed: 26706447]

Hanslmayr S, Aslan A, Staudigl T, Klimesch W, Herrmann CS, & Bäuml KH (2007). Prestimulus oscillations predict visual perception performance between and within subjects. Neuroimage, 37(4), 1465–1473. doi: 10.1016/j.neuroimage.2007.07.011 [PubMed: 17706433]

He BJ, Snyder AZ, Vincent JL, Epstein A, Shulman GL, & Corbetta M (2007). Breakdown of functional connectivity in frontoparietal networks underlies behavioral deficits in spatial neglect. Neuron, 53(6), 905–918. doi: 10.1016/j.neuron.2007.02.013 [PubMed: 17359924]

Heinrichs-Graham E, McDermott TJ, Mills MS, Coolidge NM, & Wilson TW (2016). Transcranial direct-current stimulation modulates offline visual oscillatory activity: A magnetoencephalography study. Cortex, 88, 19–31. doi: 10.1016/j.cortex.2016.11.016 [PubMed: 28042984]

Heinrichs-Graham E, McDermott TJ, Mills MS, Coolidge NM, & Wilson TW (2017). Transcranial direct-current stimulation modulates offline visual oscillatory activity: A magnetoencephalography study. Cortex, 88, 19–31. doi: 10.1016/j.cortex.2016.11.016 [PubMed: 28042984]

Heinrichs-Graham E, & Wilson TW (2016). Is an absolute level of cortical beta suppression required for proper movement? Magnetoencephalographic evidence from healthy aging. Neuroimage, 134, 514–521. doi:10.1016/j.neuroimage.2016.04.032 [PubMed: 27090351]

Hill AT, Fitzgerald PB, & Hoy KE (2016). Effects of Anodal Transcranial Direct Current Stimulation on Working Memory: A Systematic Review and Meta-Analysis of Findings From Healthy and Neuropsychiatric Populations. Brain Stimul, 9(2), 197–208. doi: 10.1016/j.brs.2015.10.006 [PubMed: 26597929]

Hoogenboom N, Schoffelen JM, Oostenveld R, Parkes LM, & Fries P (2006). Localizing human visual gamma-band activity in frequency, time and space. Neuroimage, 29(3), 764–773. doi:10.1016/j.neuroimage.2005.08.043 [PubMed: 16216533]

Horvath JC, Forte JD, & Carter O (2015a). Evidence that transcranial direct current stimulation (tDCS) generates little-to-no reliable neurophysiologic effect beyond MEP amplitude modulation in healthy human subjects: A systematic review. Neuropsychologia, 66, 213–236. doi:10.1016/j.neuropsychologia.2014.11.021 [PubMed: 25448853]

Horvath JC, Forte JD, & Carter O (2015b). Quantitative Review Finds No Evidence of Cognitive Effects in Healthy Populations From Single-session Transcranial Direct Current Stimulation (tDCS). Brain Stimul, 8(3), 535–550. doi: 10.1016/j.brs.2015.01.400 [PubMed: 25701175]

Hsu TY, Tseng P, Liang WK, Cheng SK, & Juan CH (2014). Transcranial direct current stimulation over right posterior parietal cortex changes prestimulus alpha oscillation in visual short-term memory task. Neuroimage, 98, 306–313. doi: 10.1016/j.neuroimage.2014.04.069 [PubMed: 24807400]

Jackson MP, Rahman A, Lafon B, Kronberg G, Ling D, Parra LC, & Bikson M (2016). Animal models of transcranial direct current stimulation: Methods and mechanisms. Clin Neurophysiol, 127(11), 3425–3454. doi: 10.1016/j.clinph.2016.08.016 [PubMed: 27693941]

Jasper HH (1958). The ten twenty electrode system of the international federation. (Vol. 10, pp. 371–375). Electroencephalography and clinical neurophysiology.

Jensen O, & Mazaheri A (2010). Shaping functional architecture by oscillatory alpha activity: gating by inhibition. Front Hum Neurosci, 4, 186. doi: 10.3389/fnhum.2010.00186 [PubMed: 21119777]

Jensen O, & Tesche CD (2002). Frontal theta activity in humans increases with memory load in a working memory task. Eur J Neurosci, 15(8), 1395–1399. [PubMed: 11994134]

Jurkiewicz MT, Gaetz WC, Bostan AC, & Cheyne D (2006). Post-movement beta rebound is generated in motor cortex: evidence from neuromagnetic recordings. Neuroimage, 32(3), 1281–1289. doi: 10.1016/j.neuroimage.2006.06.005 [PubMed: 16863693]

Kelly SP, Lalor EC, Reilly RB, & Foxe JJ (2006). Increases in alpha oscillatory power reflect an active retinotopic mechanism for distracter suppression during sustained visuospatial attention. J Neurophysiol, 95(6), 3844–3851. doi: 10.1152/jn.01234.2005 [PubMed: 16571739]

Kempe R, Huang Y, & Parra LC (2014). Simulating pad-electrodes with high-definition arrays in transcranial electric stimulation. J Neural Eng, 11(2), 026003. doi: 10.1088/1741-2560/11/2/026003 [PubMed: 24503644]

Klimesch W (2012). α-band oscillations, attention, and controlled access to stored information. Trends Cogn Sci, 16(12), 606–617. doi: 10.1016/j.tics.2012.10.007 [PubMed: 23141428]

Klimesch W, Sauseng P, & Hanslmayr S (2007). EEG alpha oscillations: the inhibition-timing hypothesis. Brain Res Rev, 53(1), 63–88. doi: 10.1016/j.brainresrev.2006.06.003 [PubMed: 16887192]

Kuo HI, Bikson M, Datta A, Minhas P, Paulus W, Kuo MF, & Nitsche MA (2013). Comparing cortical plasticity induced by conventional and high-definition 4 × 1 ring tDCS: a neurophysiological study. Brain Stimul, 6(4), 644–648. doi: 10.1016/j.brs.2012.09.010 [PubMed: 23149292]

Kurz MJ, Wiesman AI, Coolidge NM, & Wilson TW (2017). Children with Cerebral Palsy Hyper-Gate Somatosensory Stimulations of the Foot. Cereb Cortex, 1–8. doi: 10.1093/cercor/bhx144

Kwon S, Watanabe M, Fischer E, & Bartels A (2017). Attention reorganizes connectivity across networks in a frequency specific manner. Neuroimage, 144(Pt A), 217–226. doi:10.1016/j.neuroimage.2016.10.014 [PubMed: 27732887]

Lachaux JP, Rodriguez E, Martinerie J, & Varela FJ (1999). Measuring phase synchrony in brain signals. Hum Brain Mapp, 8(4), 194–208. [PubMed: 10619414]

Lafon B, Rahman A, Bikson M, & Parra LC (2017). Direct Current Stimulation Alters Neuronal Input/Output Function. Brain Stimul, 10(1), 36–45. doi: 10.1016/j.brs.2016.08.014 [PubMed: 27717601]

Landau AN, & Fries P (2012). Attention samples stimuli rhythmically. Curr Biol, 22(11), 1000–1004. doi: 10.1016/j.cub.2012.03.054 [PubMed: 22633805]

Landau AN, Schreyer HM, van Pelt S, & Fries P (2015). Distributed Attention Is Implemented through Theta-Rhythmic Gamma Modulation. Curr Biol, 25(17), 2332–2337. doi:10.1016/j.cub.2015.07.048 [PubMed: 26279231]

Liebe S, Hoerzer GM, Logothetis NK, & Rainer G (2012). Theta coupling between V4 and prefrontal cortex predicts visual short-term memory performance. Nat Neurosci, 15(3), 456–462, S451–452. doi:10.1038/nn.3038 [PubMed: 22286175]

Mancuso LE, Ilieva IP, Hamilton RH, & Farah MJ (2016). Does Transcranial Direct Current Stimulation Improve Healthy Working Memory?: A Meta-analytic Review. J Cogn Neurosci, 28(8), 1063–1089. doi: 10.1162/jocn_a_00956 [PubMed: 27054400]

Maris E, & Oostenveld R (2007). Nonparametric statistical testing of EEG- and MEG-data. J Neurosci Methods, 164(1), 177–190. doi: 10.1016/j.jneumeth.2007.03.024 [PubMed: 17517438]

Marshall L, Mölle M, Hallschmid M, & Born J (2004). Transcranial direct current stimulation during sleep improves declarative memory. J Neurosci, 24(44), 9985–9992. doi:10.1523/JNEUROSCI.2725-04.2004 [PubMed: 15525784]

Marshall TR, Esterer S, Herring JD, Bergmann TO, & Jensen O (2016). On the relationship between cortical excitability and visual oscillatory responses - A concurrent tDCS-MEG study. Neuroimage, 140, 41–49. doi: 10.1016/j.neuroimage.2015.09.069 [PubMed: 26455793]

Marshall TR, O'Shea J, Jensen O, & Bergmann TO (2015). Frontal eye fields control attentional modulation of alpha and gamma oscillations in contralateral occipitoparietal cortex. J Neurosci, 35(4), 1638–1647. doi: 10.1523/JNEUROSCI.3116-14.2015 [PubMed: 25632139]

McDermott TJ, Wiesman AI, Proskovec AL, Heinrichs-Graham E, & Wilson TW (2017). Spatiotemporal oscillatory dynamics of visual selective attention during a flanker task. Neuroimage, 156, 277–285. doi: 10.1016/j.neuroimage.2017.05.014 [PubMed: 28501539]

Muthukumaraswamy SD, & Singh KD (2013). Visual gamma oscillations: the effects of stimulus type, visual field coverage and stimulus motion on MEG and EEG recordings. Neuroimage, 69, 223–230. doi: 10.1016/j.neuroimage.2012.12.038 [PubMed: 23274186]

Nitsche MA, Nitsche MS, Klein CC, Tergau F, Rothwell JC, & Paulus W (2003). Level of action of cathodal DC polarisation induced inhibition of the human motor cortex. Clin Neurophysiol, 114(4), 600–604. [PubMed: 12686268]

Nitsche MA, & Paulus W (2000). Excitability changes induced in the human motor cortex by weak transcranial direct current stimulation. J Physiol, 527 Pt 3, 633–639. [PubMed: 10990547]

Nitsche MA, & Paulus W (2001). Sustained excitability elevations induced by transcranial DC motor cortex stimulation in humans. Neurology, 57(10), 1899–1901. [PubMed: 11723286]

Okamoto M, Dan H, Sakamoto K, Takeo K, Shimizu K, Kohno S,… Dan I (2004). Three-dimensional probabilistic anatomical cranio-cerebral correlation via the international 10–20 system oriented for transcranial functional brain mapping. Neuroimage, 21(1), 99–111. [PubMed: 14741647]

Okamoto M, & Dan I (2005). Automated cortical projection of head-surface locations for transcranial functional brain mapping. Neuroimage, 26(1), 18–28. doi: 10.1016/j.neuroimage.2005.01.018 [PubMed: 15862201]

Romei V, Brodbeck V, Michel C, Amedi A, Pascual-Leone A, & Thut G (2008). Spontaneous fluctuations in posterior alpha-band EEG activity reflect variability in excitability of human visual areas. Cereb Cortex, 18(9), 2010–2018. doi: 10.1093/cercor/bhm229 [PubMed: 18093905]

Romei V, Gross J, & Thut G (2010). On the role of prestimulus alpha rhythms over occipito-parietal areas in visual input regulation: correlation or causation? J Neurosci, 30(25), 8692–8697. doi: 10.1523/JNEUROSCI.0160-10.2010 [PubMed: 20573914]

Romei V, Rihs T, Brodbeck V, & Thut G (2008). Resting electroencephalogram alpha-power over posterior sites indexes baseline visual cortex excitability. Neuroreport, 19(2), 203–208. doi: 10.1097/WNR.0b013e3282f454c4 [PubMed: 18185109]

Ruffini G, Fox MD, Ripolles O, Miranda PC, & Pascual-Leone A (2014). Optimization of multifocal transcranial current stimulation for weighted cortical pattern targeting from realistic modeling of electric fields. Neuroimage, 89, 216–225. doi: 10.1016/j.neuroimage.2013.12.002 [PubMed: 24345389]

Siegel M, Donner TH, Oostenveld R, Fries P, & Engel AK (2007). High-frequency activity in human visual cortex is modulated by visual motion strength. Cereb Cortex, 17(3), 732–741. doi:10.1093/cercor/bhk025 [PubMed: 16648451]

Spaak E, de Lange FP, & Jensen O (2014). Local entrainment of alpha oscillations by visual stimuli causes cyclic modulation of perception. J Neurosci, 34(10), 3536–3544. doi:10.1523/JNEUROSCI.438513.2014 [PubMed: 24599454]

Szczepanski SM, Crone NE, Kuperman RA, Auguste KI, Parvizi J, & Knight RT (2014). Dynamic changes in phase-amplitude coupling facilitate spatial attention control in frontoparietal cortex. PLoS Biol, 12(8), e1001936. doi: 10.1371/journal.pbio.1001936 [PubMed: 25157678]

Tallon-Baudry C, Bertrand O, Henaff MA, Isnard J, & Fischer C (2005). Attention modulates gamma-band oscillations differently in the human lateral occipital cortex and fusiform gyrus. Cereb Cortex, 15(5), 654–662. doi: 10.1093/cercor/bhh167 [PubMed: 15371290]

Taulu S, & Simola J (2006). Spatiotemporal signal space separation method for rejecting nearby interference in MEG measurements. Phys Med Biol, 51(7), 1759–1768. doi: 10.1088/0031-9155/51/7/008 [PubMed: 16552102]

van Dijk H, Schoffelen JM, Oostenveld R, & Jensen O (2008). Prestimulus oscillatory activity in the alpha band predicts visual discrimination ability. J Neurosci, 28(8), 1816–1823. doi:10.1523/JNEUROSCI.1853-07.2008 [PubMed: 18287498]

Verbruggen F, Aron AR, Stevens MA, & Chambers CD (2010). Theta burst stimulation dissociates attention and action updating in human inferior frontal cortex. Proc Natl Acad Sci U S A, 107(31), 13966–13971. doi: 10.1073/pnas.1001957107 [PubMed: 20631303]

Vidal JR, Chaumon M, O'Regan JK, & Tallon-Baudry C (2006). Visual grouping and the focusing of attention induce gamma-band oscillations at different frequencies in human magnetoencephalogram signals. J Cogn Neurosci, 18(11), 1850–1862. doi: 10.1162/jocn.2006.18.11.1850 [PubMed: 17069476]

Wiesman AI, Heinrichs-Graham E, Coolidge NM, Gehringer JE, Kurz MJ, & Wilson TW (2016). Oscillatory dynamics and functional connectivity during gating of primary somatosensory responses. J Physiol. doi: 10.1113/JP273192

Wiesman AI, Heinrichs-Graham E, McDermott TJ, Santamaria PM, Gendelman HE, & Wilson TW (2016). Quiet connections: Reduced fronto-temporal connectivity in nondemented Parkinson's Disease during working memory encoding. Hum Brain Mapp. doi: 10.1002/hbm.23237

Wiesman AI, Heinrichs-Graham E, Proskovec AL, McDermott TJ, & Wilson TW (2017). Oscillations during observations: Dynamic oscillatory networks serving visuospatial attention. Hum Brain Mapp, 38(10), 5128–5140. doi: 10.1002/hbm.23720 [PubMed: 28714584]

Wiesman AI, O'Neill J, Mills MS, Robertson KR, Fox HS, Swindells S, & Wilson TW (2018). Aberrant occipital dynamics differentiate HIV-infected patients with and without cognitive impairment. Brain. doi: 10.1093/brain/awy097

Wilson TW, Heinrichs-Graham E, & Becker KM (2014). Circadian modulation of motor-related beta oscillatory responses. Neuroimage, 102 Pt 2, 531–539. doi:10.1016/j.neuroimage.2014.08.013 [PubMed: 25128712]

Wilson TW, Kurz MJ, & Arpin DJ (2014). Functional specialization within the supplementary motor area: a fNIRS study of bimanual coordination. Neuroimage, 85 Pt 1, 445–450. doi:10.1016/j.neuroimage.2013.04.112 [PubMed: 23664948]

Wilson TW, McDermott TJ, Mills MS, Coolidge NM, & Heinrichs-Graham E (2018). tDCS Modulates Visual Gamma Oscillations and Basal Alpha Activity in Occipital Cortices: Evidence from MEG. Cereb Cortex, 28(5), 1597–1609. doi: 10.1093/cercor/bhx055 [PubMed: 28334214]

Wilson TW, Proskovec AL, Heinrichs-Graham E, O'Neill J, Robertson KR, Fox HS, & Swindells S (2017). Aberrant Neuronal Dynamics during Working Memory Operations in the Aging HIV-Infected Brain. Sci Rep, 7, 41568. doi: 10.1038/srep41568 [PubMed: 28155864]

Worden MS, Foxe JJ, Wang N, & Simpson GV (2000). Anticipatory biasing of visuospatial attention indexed by retinotopically specific alpha-band electroencephalography increases over occipital cortex. J Neurosci, 20(6), RC63. [PubMed: 10704517]

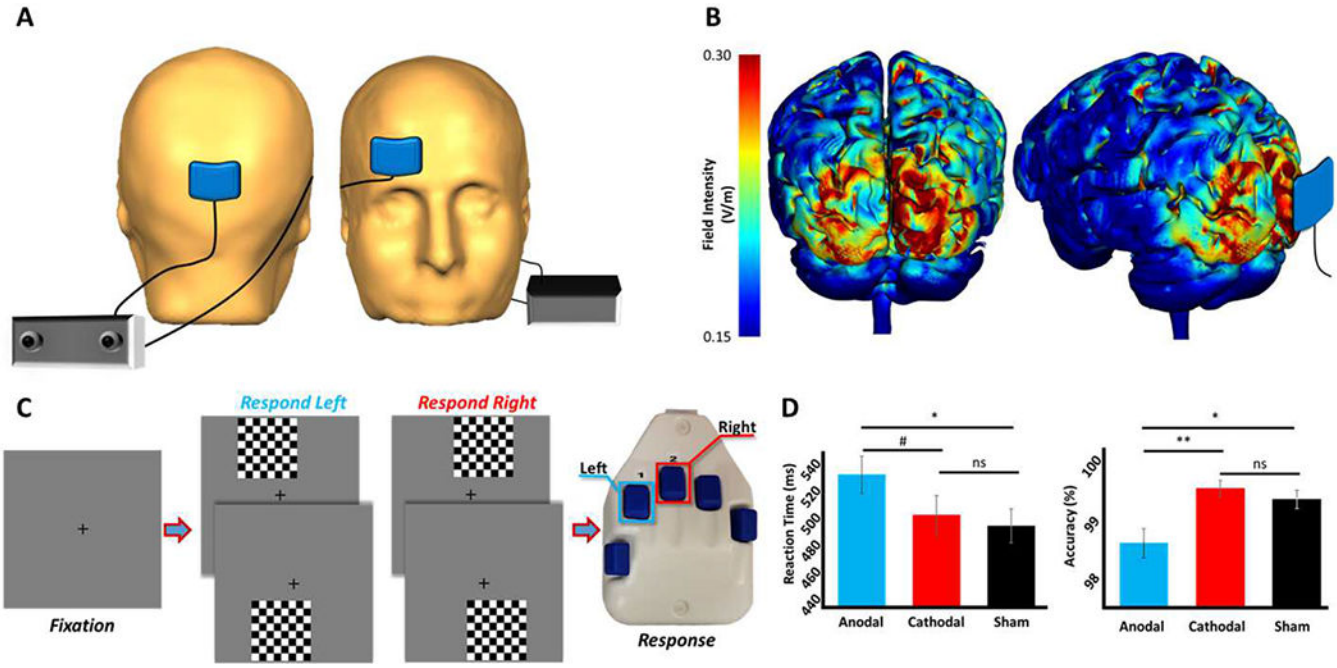

Figure 1.

Experimental paradigm, current distribution modeling, and behavioral results. (A) Spatial representation of the stimulation electrodes. (B) Results of the current distribution modeling in occipital cortices for the stimulation montage, represented as field intensity (V/m). (C) An illustration of the visuospatial discrimination task paradigm. (D) Behavioral results from the visuospatial task, with stimulation condition denoted on the x-axes. Reaction time (in milliseconds) is displayed on the y-axis of the graph on the left, and accuracy (in % correct) is displayed on the y-axis of the graph to the right.$^{\#}p < .10$, $*p < .05$, $**p < .01$

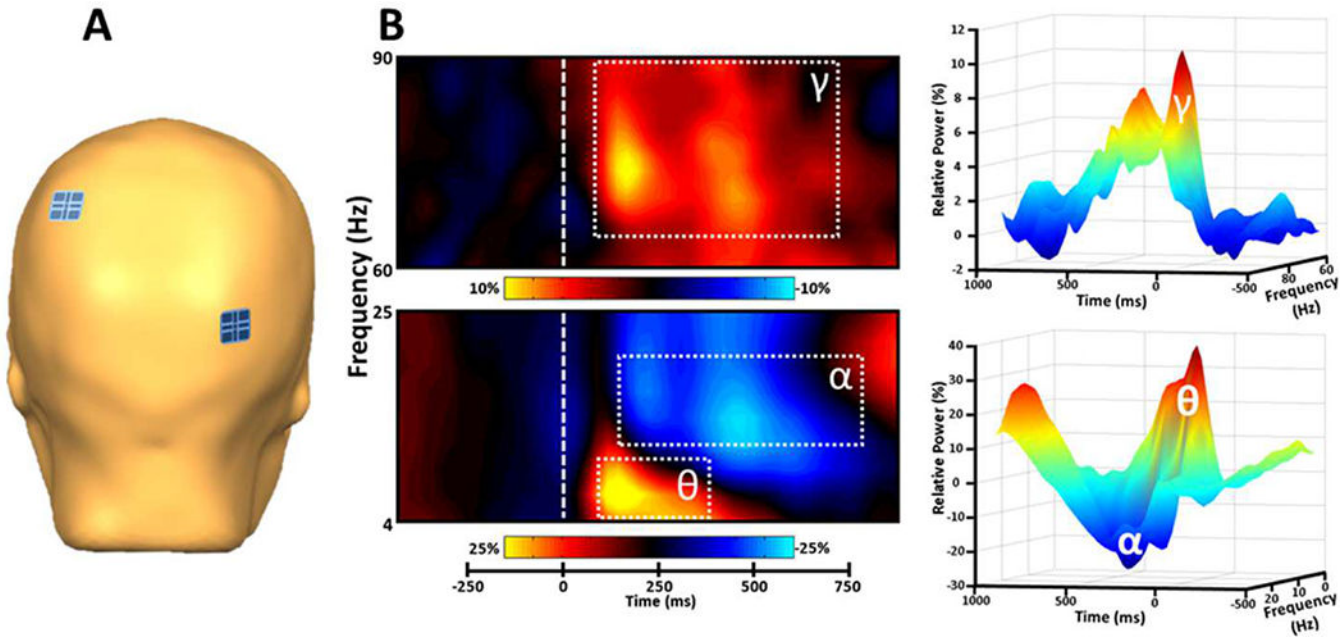

Figure 2.

Spectral time course of occipital neural responses at the sensor level. (A) Spatial location of the representative sensors used for (B), with the gamma response represented in the sensor on the lower-right, and the alpha and theta responses represented in the sensor on the upper-left. (B) Two depictions of occipital spectral responses to the visual processing task. For the spectrograms on the left, time (in milliseconds) is denoted on the x-axes, with 0 ms defined as the onset of the visual stimulus, and frequency (in Hz) shown on the y-axes. The color scale bar for percent change is shown beneath each plot. The 3D spectrograms on the right display time on the x-axes, relative power (in %) on the y-axes, and frequency on the z-axes. All signal power data is expressed as a percent difference from baseline (−400 to 0 ms). All spectrograms represent group-averaged data from gradiometer sensors that were representative of the significant neural response in each region. The same sensors were selected in all

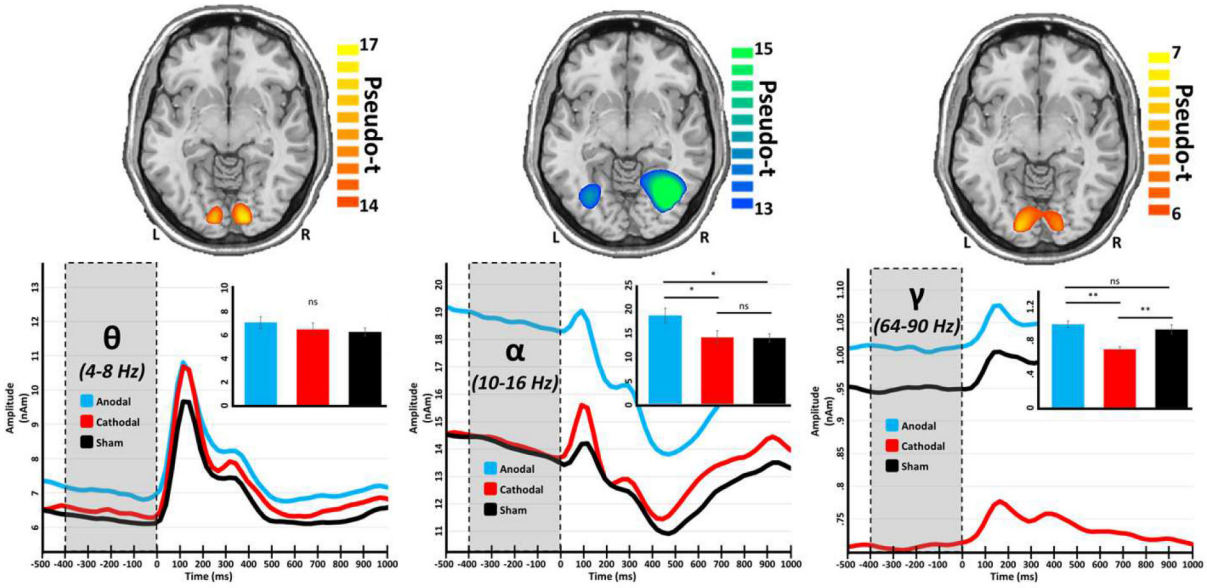

Figure 3.

The polarity of tDCS differentially affects baseline amplitude in a frequency-specific manner. Axial slices (top) show group mean beamformer images of the bilateral visual responses at each frequency. The respective color legend for each image is displayed to the right. Peak voxel time series for each set of visual responses were extracted, averaged across hemisphere, and are displayed below their respective spatial map, with time (in milliseconds) denoted on the x-axes, and absolute amplitude (in nAm) denoted on the y-axes. Shaded regions (from −400 to 0 ms) represent the baseline period, over which average values were obtained for each participant. Inlaid bar graphs represent these baseline values averaged across participants per stimulation group, with significance levels of post-hoc analyses indicated by asterisks above the bars. *$p < .05$, **$p < .01$

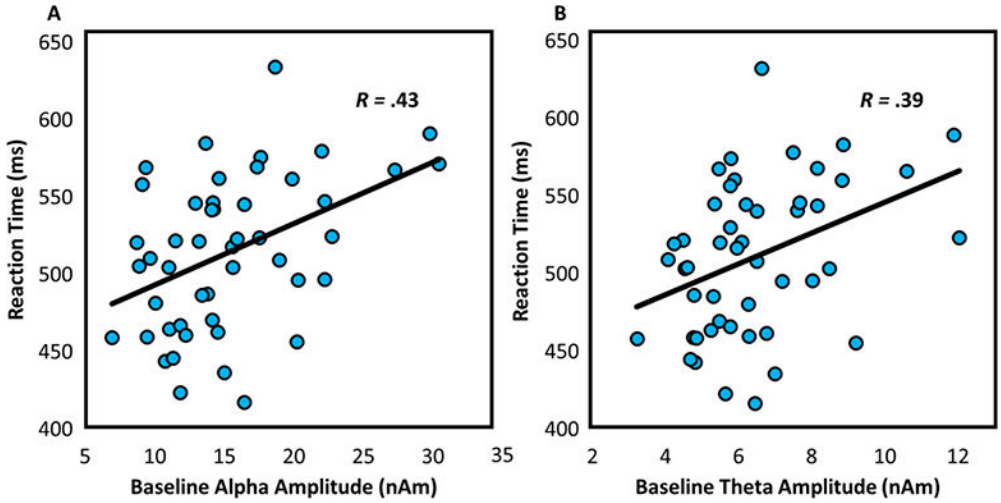

Figure 4.

Spontaneous (basal) alpha and theta during the baseline predicts behavior. Scatterplots displaying the relationship between reaction time on the y-axes and spontaneous alpha activity (in nAm) during the baseline on the x-axis of (A), and spontaneous theta (in nAm) during the baseline on the x-axis of (B). The respective line of best fit and *R* value for each simple regression is overlaid on each plot.

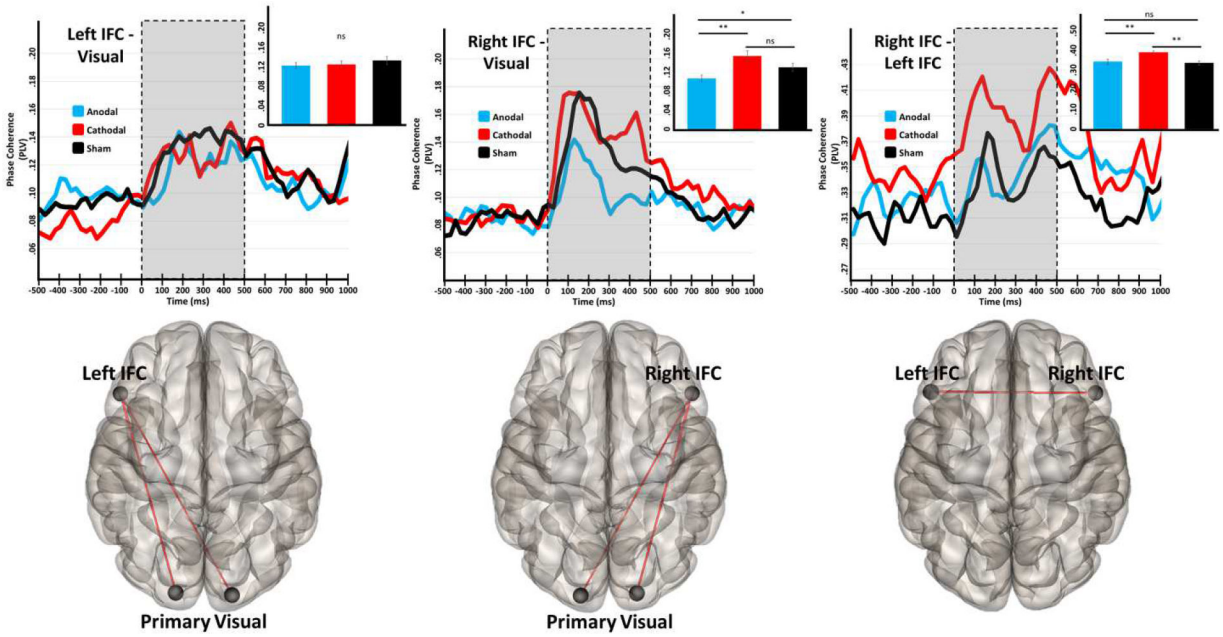

Figure 5.

tDCS selectively modulates the strength of functional connectivity among prefrontal and visual regions in the theta band. The glass brains under each plot represent the functional connections interrogated. Time series represent dynamic functional connectivity for each stimulation group, with time (in milliseconds) denoted on the x-axes and phase locking value (PLV) represented on the y-axes. In the fronto-occipital plots (left and middle panels) the time series has been averaged over the two pathways shown in the glass brain below. Shaded regions represent the "task-active" period over which PLV was averaged for each participant prior to statistical analyses, and inlaid bar graphs represent the average PLV for each stimulation condition. Significance levels of post-hoc statistical tests are indicated by asterisks above. *$p < .05$, **$p < .01$

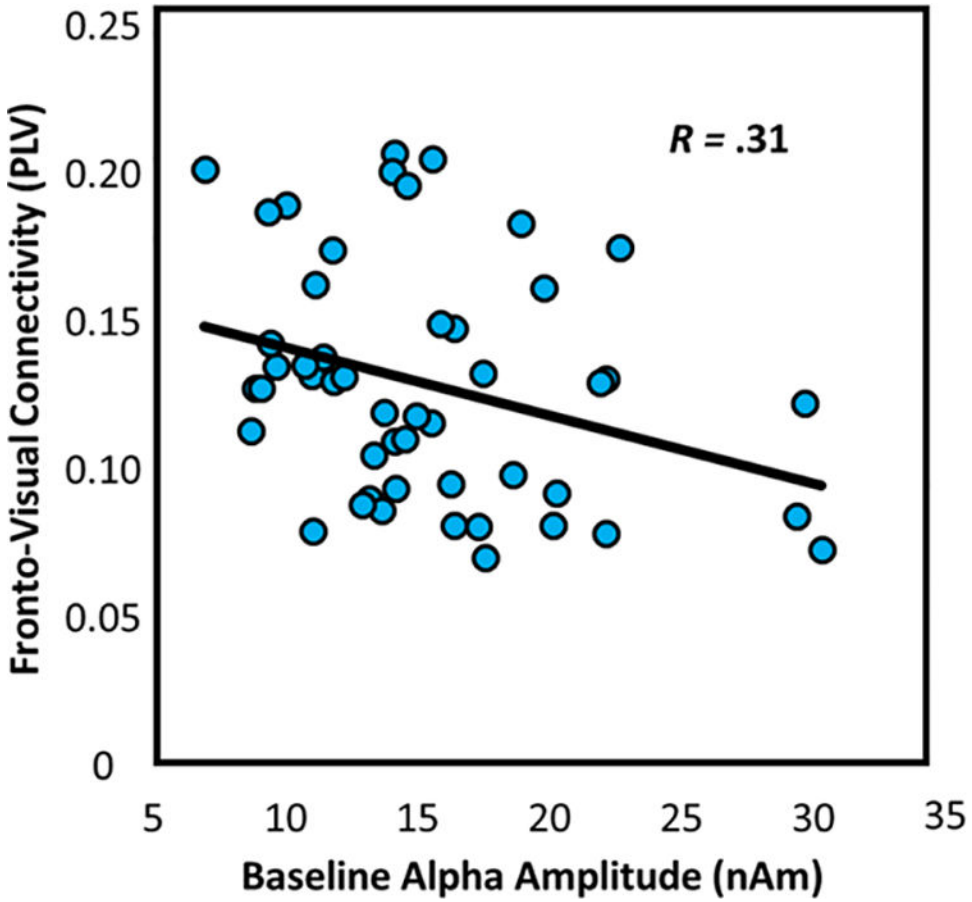

Figure 6.

Spontaneous (basal) alpha activity at baseline predicts theta functional connectivity. Scatterplots displaying the relationship between spontaneous alpha amplitude (in nAm) during the baseline on the x-axis and fronto-visual connectivity (in PLV) on the y-axis. The respective line of best fit and *R* value for the simple regression is overlaid on the plot.